

# Solid helium at high pressure: A path-integral Monte Carlo simulation

Carlos P. Herrero

*Instituto de Ciencia de Materiales, Consejo Superior de Investigaciones Científicas (CSIC), Campus de Cantoblanco, 28049 Madrid, Spain*

(Dated: February 6, 2008)

Solid helium ( $^3\text{He}$  and  $^4\text{He}$ ) in the hcp and fcc phases has been studied by path-integral Monte Carlo. Simulations were carried out in the isothermal-isobaric ( $NPT$ ) ensemble at pressures up to 52 GPa. This allows one to study the temperature and pressure dependences of isotopic effects on the crystal volume and vibrational energy in a wide parameter range. The obtained equation of state at room temperature agrees with available experimental data. The kinetic energy,  $E_k$ , of solid helium is found to be larger than the vibrational potential energy,  $E_p$ . The ratio  $E_k/E_p$  amounts to about 1.4 at low pressures and decreases as the applied pressure is raised, converging to 1, as in a harmonic solid. Results of these simulations have been compared with those yielded by previous path integral simulations in the  $NVT$  ensemble. The validity range of earlier approximations is discussed.

PACS numbers: 67.80.-s, 62.50.+p, 65.40.De, 05.10.Ln

## I. INTRODUCTION

Structural and thermodynamic properties of solid helium have been of continuous interest in condensed matter physics because of its quantum nature and electronic simplicity. In fact, solid helium is in many respects an archetypal “quantum solid,” where zero-point energy and associated anharmonic effects are appreciably larger than in most known solids. This gives rise to peculiar properties, whose understanding has presented a challenge for elaborated theories and modelling from a microscopic standpoint [1]. Among these properties, the behavior of condensed helium at high density has received much attention. In fact, diamond-anvil-cell and shock-wave experiments have allowed to study the equation of state (EOS) of solid helium up to pressures on the order of 50 GPa [2, 3, 4]. In last years, the effect of pressure on heavier rare-gas solids has also been of interest for both experimentalists [5, 6] and theorists [7, 8, 9, 10].

Anharmonic effects in solids, and in solid helium in particular, have been traditionally studied by using theoretical techniques such as quasiharmonic approximations and self-consistent phonon theories [11]. In more recent years, the Feynman path-integral formulation of statistical mechanics [12, 13] has been exploited to study thermodynamic properties of solids at temperatures lower than their Debye temperature  $\Theta_D$ , where the quantum character of the atomic nuclei is relevant. Monte Carlo sampling applied to evaluate finite-temperature path integrals allows one to carry out quantitative and nonperturbative studies of highly-anharmonic effects in solids [1].

The path-integral Monte Carlo (PIMC) technique has been used to study several properties of solid helium [1, 14, 15, 16, 17], as well as heavier rare-gas solids [18, 19, 20, 21, 22]. For helium, in particular, this method has predicted kinetic-energy values [14] and Debye-Waller factors [23] in good agreement with data derived from experiments [24, 25]. PIMC simulations

were also employed to study the isotopic shift in the helium melting pressure [15, 16]. The EOS of solid helium at  $T = 0$  has been studied by diffusion Monte Carlo in a wide density range (down to a molar volume of 15  $\text{cm}^3/\text{mol}$ ), using an accurate interatomic potential [26]. This has been done by Chang and Boninsegni [17] at finite temperatures for both solid and liquid helium, by using PIMC simulations with several interatomic potentials, and for molar volumes down to 2.6  $\text{cm}^3/\text{mol}$ . These authors suggested that the use of effective potentials including two- and three-body terms alone can be insufficient to reproduce the EOS of condensed helium, in the pressure range experimentally accessible at present.

In this paper, we study the effect of pressure on solid  $^3\text{He}$  and  $^4\text{He}$  by PIMC simulations. We employ the isothermal-isobaric ( $NPT$ ) ensemble, which allows us to consider properties of these solids along well-defined isobars. The interatomic interaction is described by a combination of two- and three-body terms, which are directly included in the simulations. This permits us to check results of earlier simulations, where the effect of three-body terms was taken into account in a perturbative way [16, 17]. By comparing results for  $^3\text{He}$  and  $^4\text{He}$ , we analyse isotopic effects on the vibrational energy and crystal volume of solid helium.

The paper is organized as follows. In Sec. II, the computational method is described. In Sec. III we present results for the equation of state, vibrational energy, and isotopic effects on the lattice parameters. Finally, Sec. IV includes a discussion of the results and the conclusions.

## II. METHOD

Equilibrium properties of solid helium in the face-centred cubic (fcc) and hexagonal close-packed (hcp) phases have been calculated by PIMC simulations in the  $NPT$  ensemble. Most of our simulations were performed on supercells of the fcc and hcp unit cells, including 500

and 432 helium atoms respectively. To check the convergence of our results with system size, some simulations were carried out for other supercell sizes, and it was found that finite-size effects for  $N > 400$  atoms are negligible for the quantities studied here (they are smaller than the error bars).

Helium atoms have been treated as quantum particles interacting through an effective interatomic potential, composed of a two-body and a three-body part. For the two-body interaction, we have taken the potential developed by Aziz *et al.* [27] (the so-called HFD-B3-FCI1 potential). For the three-body part we have employed a Bruch-McGee-type potential [28, 29], which includes the exchange three-body interaction and a triple-dipole Axilrod-Teller interaction. For most of the simulations presented below, the parameters employed for the three-body terms were those given by Loubeyre [29], but with the parameter  $A$  in the attractive exchange interaction rescaled by a factor 2/3 (as suggested in Ref. [16], and giving  $A = 20.43$  au).

In the path-integral formulation of statistical mechanics, the partition function is evaluated through a discretization of the density matrix along cyclic paths, composed of a finite number  $L$  (Trotter number) of “imaginary-time” steps [12, 13]. In the numerical simulations, this discretization gives rise to the appearance of  $L$  replicas for each quantum particle. Thus, the practical implementation of this method relies on an isomorphism between the quantum system and a classical one, obtained by replacing each quantum particle by a cyclic chain of  $L$  classical particles, connected by harmonic springs with a temperature-dependent constant. Details on this computational method can be found elsewhere [1, 30, 31].

Our simulations were based on the so-called “primitive” form of PIMC [32, 33]. For interatomic potentials including only two-body terms, effective forms for the density matrix have been developed, which allow one to reduce efficiently the Trotter number, thereby simplifying appreciably the calculation [16]. Such a simplification is not possible here, since we consider explicitly three-body terms in the simulations. Quantum exchange effects between atomic nuclei were not considered, as they are negligible for solid helium at the pressures and temperatures studied here. (This should be valid as long as there are no vacancies and  $T$  is greater than the exchange frequency  $\sim 10^{-6}$  K [1].) The dynamic effect of the interactions between nearest and next-nearest neighbours is explicitly considered. The effect of interactions beyond next-nearest neighbours is taken into account by a static-lattice approximation [19, 34], which was employed earlier in PIMC simulations of rare-gas solids [7, 22]. We have checked that including dynamical correlations between more distant atom shells does not change the results presented below. For the energy we have used the “crude” estimator, as defined in Refs. [32, 33]. All calculations have been performed using our PIMC code [35], that has been employed earlier to study various types of

solids [22, 31, 36, 37].

Sampling of the configuration space has been carried out by the Metropolis method at pressures  $P \leq 52$  GPa, and temperatures between 25 K and the melting temperature of the solid at each considered pressure. A simulation run proceeds via successive Monte Carlo steps. In each step, the replica coordinates are updated according to three different kinds of sampling schemes: (1) Sequential trial moves of the individual replica coordinates; (2) trial moves of the center of gravity of the cyclic paths, keeping unaltered the shape of each path, and (3) trial changes on the logarithm of the volume of the simulation cell. For given temperature and pressure, a typical run consisted of  $10^4$  Monte Carlo steps for system equilibration, followed by  $10^5$  steps for the calculation of ensemble average properties. Other technical details are the same as those used in Refs. [22, 38].

To have a nearly constant precision for the simulation results at different temperatures, we have taken a Trotter number that scales as the inverse temperature. At a given  $T$ , the value of  $L$  required to obtain convergence of the results depends on the Debye temperature  $\Theta_D$  of the considered solid (higher  $\Theta_D$  needs larger  $L$ ). Since vibrational frequencies (and the associated Debye temperature) increase as the applied pressure is raised,  $L$  has to be increased accordingly. Thus, we have taken  $LT = 4000$  K for  ${}^3\text{He}$  and 3000 K for  ${}^4\text{He}$ , which were found to be sufficient for simulations of the corresponding solids at the pressures considered here ( $P \leq 52$  GPa). This means that, for solid  ${}^3\text{He}$  at  $T = 25$  K, we have  $L = 160$  and then the computational time required to carry out a PIMC simulation for  $N = 500$  helium atoms is equivalent to a classical Monte Carlo simulation of  $LN = 80000$  atoms (assuming the same number of simulation steps).

### III. RESULTS

#### A. Crystal volume

Shown in Fig. 1 is the pressure dependence of the crystal volume for solid  ${}^4\text{He}$  at 300 K. Open symbols represent results of PIMC simulations with different interatomic potentials: (a) only two-body interactions with an Aziz-type potential [27] (squares); (b) two-body interactions as in Ref. [27] plus three-body terms as in Ref. [29] (diamonds); (c) the same two-body potential and three-body interaction with the exchange part rescaled by 2/3, as proposed in Ref. [16] (circles). For comparison, we also present results derived from PIMC simulations in the  $NVT$  ensemble [17], with the exchange interaction rescaled by the same factor 2/3 (triangles). Filled symbols indicate experimental results obtained by Mao *et al.* [3] (filled circles) and Loubeyre *et al.* [4] (filled squares). Our simulation data show that the interatomic potential (c) gives results for the equation of state of solid  ${}^4\text{He}$  close to the experimental data. The only consideration of two-body terms predicts, for a given

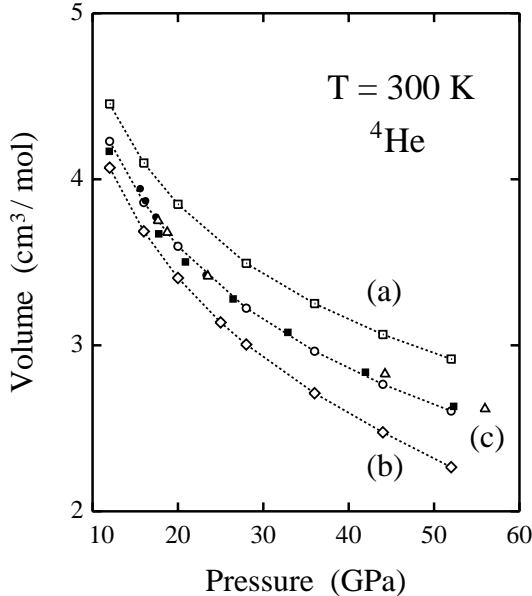


FIG. 1: Equation of state pressure-volume of hcp  ${}^4\text{He}$  at 300 K, as derived from PIMC simulations for different interatomic potentials. (a) Open squares: only two-body interactions with an Aziz-type potential [27]; (b) open diamonds: two-body terms as in Ref. [27] and three-body interactions, as defined in Ref. [29]; (c) open circles: same potential as (b), but with the exchange three-body interaction rescaled by 2/3. Error bars of the simulation results are less than the symbol size. Dotted lines are guides to the eye. Open triangles show earlier results obtained from PIMC simulations in the  $NVT$  ensemble [17], with the attractive exchange interaction rescaled as in (c). Black symbols show experimental data obtained by Mao *et al.* [3] (filled circles) and Loubeire *et al.* [4] (filled squares).

applied pressure, a crystal volume larger than the experimental one. On the contrary, consideration of both two- and three-body terms derived from *ab initio* calculations underestimates the volume of solid helium. This is in line with results obtained earlier from PIMC simulations in the  $NVT$  ensemble in Refs. [16, 17]. These authors introduced the three-body terms not directly in the simulations, but calculated in a perturbative way their contribution to thermodynamic averages from configurations obtained in PIMC simulations. In Fig. 1 (open circles and triangles) we observe that our  $NPT$  simulations give the same results as those obtained earlier in the  $NVT$  ensemble [17] for pressures lower than 30 GPa. However, at higher pressures both sets of results differ appreciably, and for a given  $P$  the procedure employed in Ref. [17] yields a volume larger than that obtained here.

Our results with the effective interatomic potential (c) follow closely the experimental ones, even at the highest pressures considered here, although they seem to become lower than the later as pressure rises. However, taking into account the dispersion of experimental points and the error bars of the simulation data, differences between both sets of data are not enough to invalidate the accuracy of the effective potential (c) in the pressure range

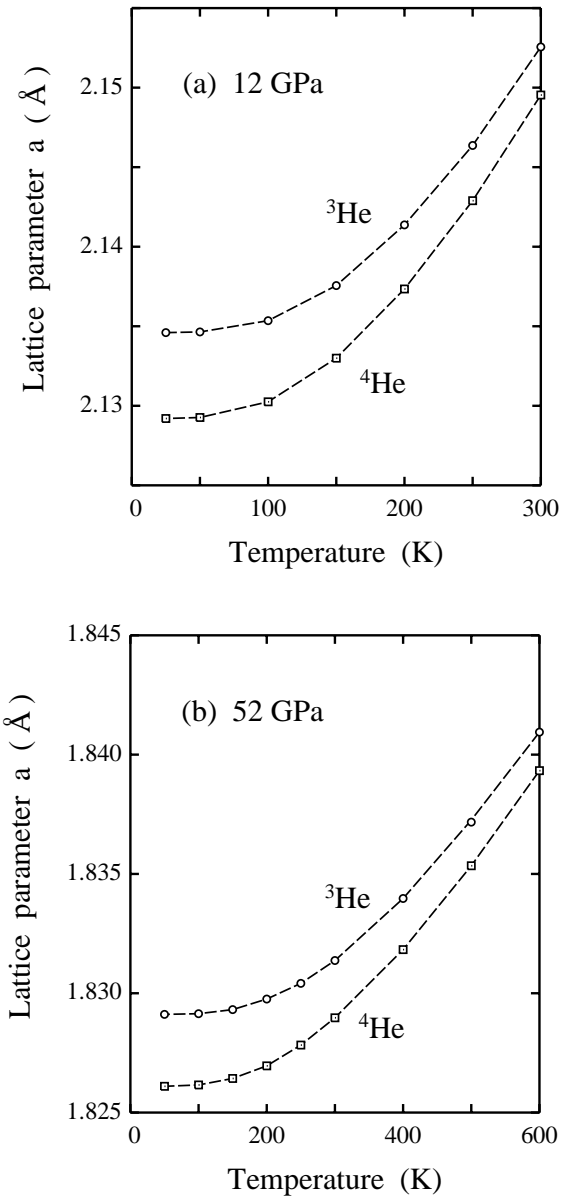


FIG. 2: Temperature dependence of the lattice parameter  $a$  of hcp helium, derived from PIMC simulations at two different pressures: (a) 12 GPa and (b) 52 GPa. Squares and circles indicate results for  ${}^4\text{He}$  and  ${}^3\text{He}$ , respectively. Error bars are smaller than the symbol size. Dashed lines are guides to the eye.

studied here. This contrasts with the conclusions presented by Chang and Boninsegni [17], who argued that two- and three-body terms alone may be insufficient to reproduce quantitatively the EOS of condensed helium at pressures on the order of 50 GPa. In fact, for molar volumes smaller than  $3 \text{ cm}^3/\text{mol}$ , these authors found pressures larger than the experimental ones (see Fig. 1). In view of these results, in the remainder of the paper we will employ only the interaction potential (c) (with the exchange three-body part of Ref. [29] rescaled by 2/3).

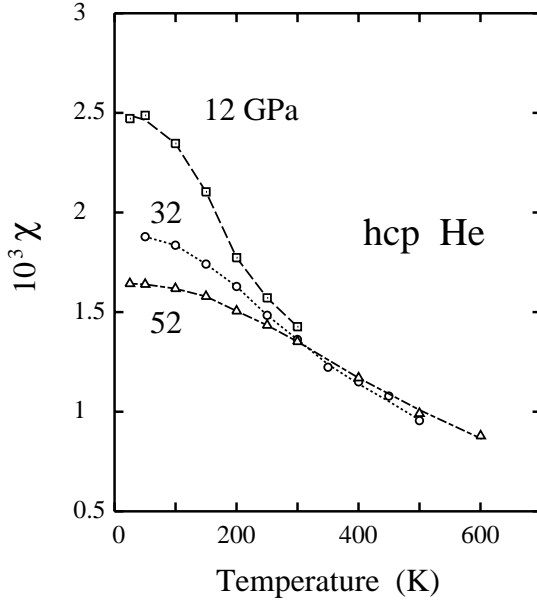


FIG. 3: Isotopic effect on the lattice parameter  $a$  of hcp helium, as obtained from PIMC simulations. Shown is the parameter  $\chi = (a_3 - a_4)/a_4$  as a function of temperature for three different pressures: squares, 12 GPa; circles, 32 GPa; triangles, 52 GPa. Error bars are on the order of the symbol size. Lines are guides to the eye.

In Fig. 2 we present the temperature dependence of the lattice parameter  $a$  for hcp helium at two pressures: (a) 12 GPa and (b) 52 GPa. Squares and circles represent results of our PIMC simulations for  ${}^4\text{He}$  and  ${}^3\text{He}$ , respectively. Note the different vertical and horizontal scales in (a) and (b). As expected, the difference  $a_3 - a_4$  between lattice parameters of  ${}^3\text{He}$  and  ${}^4\text{He}$  at a given pressure decreases as the temperature is raised (at high  $T$  the solid becomes “more classical”).

To quantify the isotopic effect on the linear dimensions of solid helium, we employ the parameter  $\chi = (a_3 - a_4)/a_4$ , which measures the relative difference between lattice parameters of solid  ${}^3\text{He}$  and  ${}^4\text{He}$ . This parameter  $\chi$  is displayed in Fig. 3 as a function of temperature for three different pressures: 12 (squares), 32 (circles), and 52 GPa (triangles). For each pressure, results are shown for temperatures at which the considered solids were stable along the PIMC simulations. At low  $T$ , the parameter  $\chi$  is larger for lower pressure, and values obtained for different pressures approach each other as the temperature rises. At  $T > 300$  K, we find that  $\chi$  is larger for  $P = 52$  GPa than for 32 GPa. This does not mean that the difference  $a_3 - a_4$  is larger at 52 GPa, but is a consequence of the normalization by  $a_4$ , which is clearly smaller at higher pressure.

The difference  $a_3 - a_4$  is largest at small pressures and low temperatures, where quantum effects are most prominent. For a given solid, quantum effects on the crystal size can be measured by the difference  $\Delta a = a - a_{\text{cl}}$  between the actual lattice parameter  $a$  and that obtained

for a “classical” crystal of point particles,  $a_{\text{cl}}$ . This difference decreases for increasing atomic mass and temperature [19, 36]. From our PIMC simulations at  $T = 25$  K and a relatively low pressure of 0.3 GPa, we found an increase in the linear size of solid  ${}^3\text{He}$  and  ${}^4\text{He}$  of 8.2 and 7.2% with respect to the classical crystal at zero temperature. For comparison, we note that the “zero-point expansion” for heavier rare gases causes a relative increase of 4.1% and 1.2% in the lattice parameter of fcc Ne and Ar, respectively [38].

## B. Energy

For a given interatomic potential, the internal energy of a solid,  $E(V, T)$ , at volume  $V$  and temperature  $T$  can be written as:

$$E(V, T) = E_{\text{min}}(V) + E_{\text{vib}}(V, T), \quad (1)$$

where  $E_{\text{min}}(V)$  is the potential energy for the (classical) crystal at  $T = 0$  with point atoms on their lattice sites, and  $E_{\text{vib}}(V, T)$  is the vibrational energy. Since we are working here in the isothermal-isobaric ensemble, the volume is implicitly given by the applied pressure. At finite temperatures,  $V$  changes with  $T$  due to thermal expansion, and for real (quantum) solids, the crystal volume depends on quantum effects, which also contribute to expand the crystal with respect to the classical expectancy (mainly at low  $T$ ). Thus, the volume  $V$  in Eq. (1) is an implicit function of  $P$  and  $T$ , i.e.,  $V = V(P, T)$ .

The vibrational energy,  $E_{\text{vib}}(V, T)$ , depends explicitly on both,  $V$  and  $T$ , and can be obtained by subtracting the energy  $E_{\text{min}}(V)$  from the internal energy. In this way, path-integral Monte Carlo simulations allow one to obtain separately the kinetic,  $E_k$ , and potential energy,  $E_p$ , associated to the lattice vibrations:  $E_{\text{vib}} = E_k + E_p$ .

In Fig. 4 we show the kinetic energy of solid helium (hcp phase) as a function of temperature for  $P = 12$  and 52 GPa. Open symbols correspond to  ${}^4\text{He}$  and filled symbols to  ${}^3\text{He}$ . At 52 GPa, the low-temperature kinetic energy of solid  ${}^4\text{He}$  is found to be 56 meV/atom, to be compared with 8.3 meV/atom obtained for the fcc phase at 25 K and low pressure ( $P = 0.3$  GPa, giving a molar volume of  $9.95 \text{ cm}^3/\text{mol}$ ). This value of  $E_k$  is similar to those obtained earlier from PIMC simulations in the  $NVT$  ensemble at temperatures close to 25 K and molar volumes around  $10 \text{ cm}^3/\text{mol}$  [23].

At low temperature the ratio  $E_k^3/E_k^4$  between the kinetic energy of  ${}^3\text{He}$  and  ${}^4\text{He}$  is close to 1.155, the expected value in a harmonic model of lattice vibrations. This indicates that, irrespective of the important anharmonicity present in these solids, anharmonic shifts in  $E_k$  scale with mass approximately as in a quasiharmonic model. The ratio  $E_k^3/E_k^4$  decreases as temperature rises and quantum effects are less important. At the highest simulated temperatures (300 K for  $P = 12$  GPa and 600 K for 52 GPa) we find  $E_k^3/E_k^4 \approx 1.05$ , still clearly larger than the classical limit:  $E_k^3/E_k^4 \rightarrow 1$ .

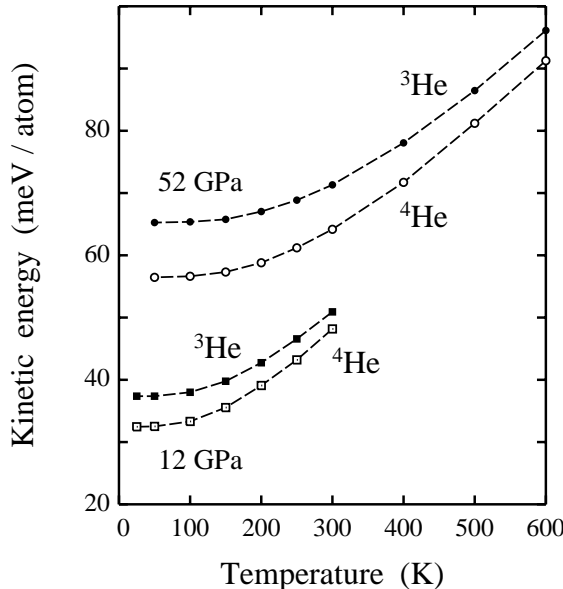


FIG. 4: Temperature dependence of the kinetic energy of hcp solid helium at two different pressures, as derived from PIMC simulations:  $P = 12$  GPa (squares) and  $52$  GPa (circles). Open and filled symbols correspond to  $^4\text{He}$  and  $^3\text{He}$ , respectively. Error bars of the simulation results are less than the symbol size. Dashed lines are guides to the eye.

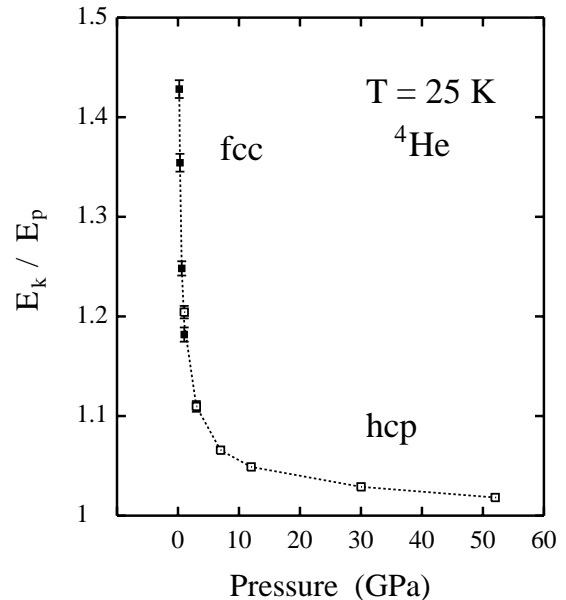


FIG. 5: Kinetic-to-potential energy ratio,  $E_k/E_p$ , for solid  $^4\text{He}$  as a function of applied pressure at  $T = 25$  K. Black and open symbols correspond to fcc and hcp phases, respectively. Error bars, where not shown, are smaller than the symbol size.

#### IV. DISCUSSION

The anharmonicity of the lattice vibrations is clearly noticeable when one compares the kinetic and potential energy of solid helium. From our PIMC simulations, we have found in all cases considered here that the vibrational potential energy  $E_p$  is smaller than the kinetic energy  $E_k$ . Shown in Fig. 5 is the ratio  $E_k/E_p$  for  $^4\text{He}$  as a function of pressure at 25 K. We have included in this figure results for fcc (low pressure) and hcp helium (high pressure). The kinetic-to-potential energy ratio decreases with increasing pressure; first it goes down fast for pressures lower than 5 GPa, and then it decreases slower at higher pressures, approaching the value  $E_k/E_p = 1$ , characteristic of harmonic vibrations. We note that the fact  $E_k > E_p$  has been also found for solids of heavier rare gases from PIMC simulations [19, 22, 38].

For solid  $^4\text{He}$  at low pressure, we find that  $E_k$  is larger than  $E_p$  by about 40%. This important difference between  $E_k$  and  $E_p$  reflects the large anharmonicity of lattice vibrations in this solid. For comparison, we mention that these energies differ by about 20% and 7% for solid neon and argon, respectively [22, 38]. These numbers are very large when compared with covalent or metallic solids, and are due to the weakness of van der Waals-type bonds, which allows for a large amplitude of the atomic vibrations.

Path-integral Monte Carlo simulations are well suited to study quantum effects on structural and thermodynamic properties of solids. These effects are particularly important for solid helium, where isotopic effects are relevant, as manifested in differences between crystal volume and vibrational energies of solid  $^3\text{He}$  and  $^4\text{He}$ . The PIMC method enables us to study phonon-related properties without the assumptions of quasiharmonic or self-consistent phonon approximations, and to study anharmonic effects in solids in a nonperturbative way. This method allows us to separate the kinetic and potential contributions to the vibrational energy of a given solid, and quantify the anharmonicity of the lattice vibrations, which together with zero-point motion give rise to isotopic effects.

PIMC simulations yield in principle “exact” values for measurable properties of many-body quantum problems, with an accuracy limited by the imaginary-time step (Trotter number) and the statistical error of the Monte Carlo sampling. Thus, the effective interatomic potential employed here gives a good description of structural and thermodynamic properties of solid helium up to pressures on the order of those presently achieved in experiments. In particular, the equation of state  $P$ - $V$  is well described by this potential in the pressure range considered here ( $P \lesssim 50$  GPa), even though it is partially an empirical potential, in the sense that the attractive three-body part was rescaled *ad hoc* from the fit to *ab initio* calculations. Explicit consideration of three-body terms in

PIMC simulations makes the computation times much longer, in comparison with simulations including only two-body terms. But this has allowed us to check the validity limit of some approximations made earlier in this kind of calculations, such as including the effect of three-body terms in a perturbative way (from configurations obtained in PIMC simulations) [16, 17]. As a result, this approximation yields at  $P < 30$  GPa an EOS indistinguishable within error bars from that obtained here. At higher pressures, however, it predicts volumes larger than those found in the present work (and in experiment).

Due to the large anharmonicity of lattice vibrations in solid helium, the isotopic effect on the crystal volume is important. At low temperatures, the dependence of the crystal volume on isotopic mass is related to the zero-point lattice expansion. The magnitude of this isotopic effect decreases appreciably as temperature or pressure are raised. Nevertheless, we emphasize that it is still measurable at the highest pressures considered here and at  $T$  close to the corresponding melting temperature, as shown in Fig. 3. This is in line with the observed isotopic effect on the melting temperature at low pressure [15, 16].

Anharmonic effects in solids have been quantified earlier by comparing the kinetic and potential energies derived from PIMC simulations [19, 38]. For solid helium, and for different pressures and temperatures, we have found  $E_k > E_p$ , as for solids of heavier rare gases with Lennard-Jones-type potentials [38]. The departure of the ratio  $E_k/E_p$  from its value for a purely harmonic solid ( $E_k/E_p = 1$ ) is a measure of the overall anharmonicity of the considered solids. For given  $T$ , we have found that this energy ratio decreases as pressure is raised. Note that the ratio  $E_k/E_p$  alone does not give any information on the details of the anharmonicity of the vibrational modes, but gives a quantitative measure of the overall anharmonicity of a given solid. In particular, it is well suited to compare the anharmonicity of similar materials. For rare-gas solids at low  $T$ ,  $E_k/E_p$  increases from 1.02 for xenon to 1.23 for neon at zero pressure [38]. This ratio is clearly higher for solid helium at low  $P$ , as shown in Fig. 5:  $E_k/E_p \approx 1.4$  for fcc  ${}^4\text{He}$  at 25 K.

It has been recently suggested that pressure causes a decrease in anharmonicity [37, 39, 40], in line with earlier observations that the accuracy of quasiharmonic approxi-

mations increases as pressure rises and the density of the material increases [41, 42]. Thus, such approximations become exact in the high-density limit [37, 42]. This is related to the fact that the ratio of the vibrational energy to the whole internal energy of the crystal decreases for increasing pressure, in spite of the increase in zero-point energy caused by the rise in vibrational frequencies. It has been also argued that at high pressures, thermodynamic properties of solids can be well described by classical calculations, i.e., dealing with the atoms as classical oscillators in a given potential [43]. This means that, at a given temperature, such a classical approach becomes more and more accurate as pressure is raised. The origin of this is similar to that described above for the success of quasiharmonic approaches. Since in this respect the lattice vibrations become less relevant as pressure rises, and eventually give a negligible contribution to the free energy of the solid, their description by a classical or a quantum model becomes unimportant for solids in the limit of very large pressures.

In summary, we have carried out PIMC simulations of solid helium in the isothermal-isobaric ensemble. In general, our results support the assumptions made in earlier calculations, where three-body terms were included in a perturbative way. In particular, the equation of state obtained here coincides at  $P \lesssim 30$  GPa with that found in calculations employing the *NVT* ensemble with that assumption. At high pressures, however, data yielded by the present PIMC simulations differ from those obtained earlier, using similar interatomic potentials. The kind of effective interatomic potentials employed here, including two- and three-body terms will probably give a poor description of solid helium at very high pressures ( $\gtrsim 60$  GPa), but seems appropriate for the pressure range in which experimental data are available at present.

## Acknowledgments

The author benefitted from discussions with R. Ramírez. This work was supported by CICYT (Spain) through Grant No. BFM2003-03372-C03-03.

---

[1] D. M. Ceperley, Rev. Mod. Phys. **67**, 279 (1995).  
 [2] A. Polian and M. Grimsditch, Europhys. Lett. **2**, 849 (1986).  
 [3] H. K. Mao, R. J. Hemley, Y. Wu, A. P. Jephcott, L. W. Finger, C. S. Zha, and W. A. Bassett, Phys. Rev. Lett. **60**, 2649 (1988).  
 [4] P. Loubeyre, R. LeToullec, J. P. Pinceaux, H. K. Mao, J. Hu, and R. J. Hemley, Phys. Rev. Lett. **71**, 2272 (1993).  
 [5] H. Shimizu, H. Tashiro, T. Kume, and S. Sasaki, Phys. Rev. Lett. **86**, 4568 (2001).  
 [6] D. Errandonea, B. Schwager, R. Boehler, and M. Ross, Phys. Rev. B **65**, 214110 (2002).  
 [7] M. Neumann and M. Zoppi, Phys. Rev. B **62**, 41 (2000).  
 [8] T. Iitaka and T. Ebisuzaki, Phys. Rev. B **65**, 012103 (2001).  
 [9] J. K. Dewhurst, R. Ahuja, S. Li, and B. Johansson, Phys. Rev. Lett. **88**, 075504 (2002).  
 [10] T. Tsuchiya and K. Kawamura, J. Chem. Phys. **117**, 5859 (2002).  
 [11] M. L. Klein and J. A. Venables, eds., *Rare Gas Solids* (Academic Press, New York, 1976).

- [12] R. P. Feynman, *Statistical Mechanics* (Addison-Wesley, New York, 1972).
- [13] H. Kleinert, *Path Integrals in Quantum Mechanics, Statistics and Polymer Physics* (World Scientific, Singapore, 1990).
- [14] D. M. Ceperley, R. O. Simmons, and R. C. Blasdell, Phys. Rev. Lett. **77**, 115 (1996).
- [15] J. L. Barrat, P. Loubeyre, and M. L. Klein, J. Chem. Phys. **90**, 5644 (1989).
- [16] M. Boninsegni, C. Pierleoni, and D. M. Ceperley, Phys. Rev. Lett. **72**, 1854 (1994).
- [17] S. Y. Chang and M. Boninsegni, J. Chem. Phys. **115**, 2629 (2001).
- [18] A. Cuccoli, A. Macchi, V. Tognetti, and R. Vaia, Phys. Rev. B **47**, 14923 (1993).
- [19] M. H. Müser, P. Nielaba, and K. Binder, Phys. Rev. B **51**, 2723 (1995).
- [20] C. Chakravarty, J. Chem. Phys. **116**, 8938 (2002).
- [21] M. Neumann and M. Zoppi, Phys. Rev. E **65**, 031203 (2002).
- [22] C. P. Herrero, Phys. Rev. B **65**, 014112 (2002).
- [23] E. W. Draeger and D. M. Ceperley, Phys. Rev. B **61**, 12094 (2000).
- [24] D. A. Arms, R. S. Shah, and R. O. Simmons, Phys. Rev. B **67**, 094303 (2003).
- [25] C. T. Venkataraman and R. O. Simmons, Phys. Rev. B **68**, 224303 (2003).
- [26] S. Moroni, F. Pederiva, S. Fantoni, and M. Boninsegni, Phys. Rev. Lett. **84**, 2650 (2000).
- [27] R. A. Aziz, A. R. Janzen, and M. R. Moldover, Phys. Rev. Lett. **74**, 1586 (1995).
- [28] L. W. Bruch and I. J. McGee, J. Chem. Phys. **59**, 409 (1973).
- [29] P. Loubeyre, Phys. Rev. Lett. **58**, 1857 (1987).
- [30] M. J. Gillan, Phil. Mag. A **58**, 257 (1988).
- [31] J. C. Noya, C. P. Herrero, and R. Ramírez, Phys. Rev. B **53**, 9869 (1996).
- [32] D. Chandler and P. G. Wolynes, J. Chem. Phys. **74**, 4078 (1981).
- [33] K. Singer and W. Smith, Mol. Phys. **64**, 1215 (1988).
- [34] A. Cuccoli, A. Macchi, G. Pedrolli, V. Tognetti, and R. Vaia, Phys. Rev. B **56**, 51 (1997).
- [35] J. C. Noya, C. P. Herrero, and R. Ramírez, unpublished.
- [36] C. P. Herrero and R. Ramírez, Phys. Rev. B **63**, 024103 (2001).
- [37] C. P. Herrero and R. Ramírez, Phys. Rev. B **71**, 174111 (2005).
- [38] C. P. Herrero, J. Phys.: Condens. Matter **15**, 475 (2003).
- [39] A. I. Karasevskii and W. B. Holzapfel, Phys. Rev. B **67**, 224301 (2003).
- [40] H. M. Lawler, E. K. Chang, and E. L. Shirley, Phys. Rev. B **69**, 174104 (2004).
- [41] E. L. Pollock, T. A. Bruce, G. V. Chester, and J. A. Krumhansl, Phys. Rev. B **5**, 4180 (1972).
- [42] B. L. Holian, W. D. Gwinn, A. C. Luntz, and B. J. Alder, J. Chem. Phys. **59**, 5444 (1973).
- [43] R. D. Etters and R. L. Danilowicz, Phys. Rev. A **9**, 1698 (1974).